ADA046952

SECURITY CLASSIFICATION OF THIS PAGE (When Data Entered)

REPORT DOCUMENTATION PAGE		READ INSTRUCTIONS BEFORE COMPLETING FORM
1. REPORT NUMBER AFAL-TR-77-36	2. GOVT ACCESSION NO.	3. RECIPIENT'S CATALOG NUMBER
4. TITLE (and Subtitle) LOW POWER HIGH DATA RATE MODULATOR		5. TYPE OF REPORT & PERIOD COVERED Final Report. 2 Jan 1975-30 Sep 1976
		6. PERFORMING ORG. REPORT NUMBER
7. AUTHOR(s) G. L. Tangonan		8. CONTRACT OR GRANT NUMBER(s) F33615-75-C-1028
9. PERFORMING ORGANIZATION NAME AND ADDRESS Hughes Research Laboratories 3011 Malibu Canyon Road Malibu, CA 90265		10. PROGRAM ELEMENT, PROJECT, TASK AREA & WORK UNIT NUMBERS Project No. 2001 02 34
11. CONTROLLING OFFICE NAME AND ADDRESS		12. REPORT DATE June 1977
38 P.		13. NUMBER OF PAGES 33
14. MONITORING AGENCY NAME & ADDRESS(if different from Controlling Office) Air Force Avionics Laboratory (DHO) Air Force Systems Command United States Air Force Wright-Patterson AFB, OH 45433		15. SECURITY CLASS. (of this report) Unclassified
		15a. DECLASSIFICATION DOWNGRADING SCHEDULE

16. DISTRIBUTION STATEMENT (of this Report)

"Approved for public release; distribution unlimited"

17. DISTRIBUTION STATEMENT (of the abstract entered in Block 20, if different from Report)

18. SUPPLEMENTARY NOTES

62204F

19. KEY WORDS (Continue on reverse side if necessary and identify by block number)

Waveguide modulators, Integrated optics, Optical Damage, Thin Film waveguides

20. ABSTRACT (Continue on reverse side if necessary and identify by block number)

The objective of this program was to develop a high-data-rate-low-power modulator for doubled Nd:YAG applications with Gigabit/sec data rate capability, 3 W drive power and capable to handle 0.5 W cw power (3.3 W peak) using integrated optics techniques. An approach to the development of this modulator has been defined. Most notable is the demonstration of optical power handling capabilities of Ti diffused LiTaO$_3$ waveguides of >300 mW with no damage and no power saturation.

DD FORM 1473 EDITION OF 1 NOV 65 IS OBSOLETE
1 JAN 73

172 607

Prism coupling efficiency of 55% input and 80% output have been achieved. The waveguide losses at 5145 Å have been measured to be 5 dB/cm. Single mode and multimode waveguides have been found by the in-diffusion process. The nature of the optical waveguide damage at room temperature and at elevated temperatures ($\square$150°C) has been studied. The high optical power densities sustained by these structures were accommodated by high temperature operation of the waveguide structures. Preliminary experiments on Bragg deflection have also been carried out.

TABLE OF CONTENTS

LIST OF ILLUSTRATIONS

INTRODUCTION AND SUMMARY

The objective of this program was to develop an optimized thin film electro-optical modulator intended for modulating digitally a mode-locked Nd:YAG laser, emitting a pulse stream at a rate of 500 megabits per second. The design goals call for a modulator capable of handling up to 500 mW average power (3.3 W peak), exhibiting sufficient bandwidth to operate at one gigabit per second, and requiring not more than 3 W driver power for a modulation depth of 95%. In addition, the optical throughput is to be no less than 60% and output beam distortion resulting from the modulator transmission characteristics should be minimal. The techniques of integrated optics provide a novel technical base for construction of such a low power high data rate modulator. Reductions in size, weight and power consumption are advantages inherent with a thin film waveguide approach to the modulator design. Of necessity is the definition of an approach toward device development based on a controllable waveguide formation process in excellent electro-optic materials (such as $LiNbO_3$ and $LiTaO_3$) and the detailed understanding of the parameters which determine the optical damage of these waveguide structures at high optical power levels. We have demonstrated during the course of this program an approach to waveguide formation in $LiTaO_3$ which preserves the excellent electro-optic properties of this material and have demonstrated that these waveguide structures can sustain high optical power densities and demonstrated that >300 mW can be coupled into these waveguides with no optical damage.

The waveguide formation technique is that of in-diffusion of Ti into $LiTaO_3$. In this process, Ti metal is diffused into $LiTaO_3$ at temperatures in the 1000 to 1300°C range for 4 to 24 hour periods. The metal is evaporated onto a polished y-cut crystal and samples with 50 to 500 Å initial Ti metal thicknesses have been studied. It has been found that

1

oxidation of the Ti metal film to TiO_2 by heating to 450°C for >4 hours in flowing O_2 before the in-diffusion process is carried out at high temperatures greatly enhances the optical quality of the waveguide layers (removes a milky appearance on the surface) and ensures reproducibility of the sample processing. This finding was crucial to the development of good quality optical waveguide layers.

The waveguide structures formed by the in-diffusion process were tested at 5145 Å (the wavelength of an argon laser) to simulate a doubled Nd:YAG laser output. The excitation of the waveguide modes of propagation was carried out using prism coupling. In this technique resonant energy transfer to optical guide modes occurs from optical fields normally totally internally reflected within the prism.[1] The prisms used were made of TiO_2 and $SrTiO_3$. Studies of the propagation at high optical power densities in these waveguide structures were made at room temperature and at slightly elevated temperatures of $\approx$ 150°C. To accomplish these tests at both temperatures a special prism coupler compatible with heating of the coupler assembly to 200°C was designed and constructed.

The optical damage phenomena occurring at room temperature and at elevated temperatures in the Ti-diffused waveguide structures are explainable by observations of optical damage in the bulk of $LiNbO_3$ and $LiTaO_3$ crystals. Local inhomogeneity of the indices of refraction are observed due to the irradiation of these crystals with high optical power densities. In the illuminated regions the extraordinary index of refraction in these regions decreases by $\approx 10^{-3}$. This causes the light to diverge, making the use of these crystals as electro-optic modulators quite difficult. It has been found that the change of the indices of refraction is due to photo-carrier excitations from transition metal impurity sites (most notable, Fe, Cu, and Mn) and oxygen vacancies which stem from reduction or the effects of off-stoichiometry. These photo-carriers, upon excitation, diffuse away from the irradiated region and are retrapped preferentially in regions of low intensity. The end result is a net space-charge pattern that is positive in regions of high intensity and negative in regions of low intensity. The fixed space charge generates an electric field that causes the index of refraction change by way of the electro-optic effect. Optical damage phenomena in optical waveguide layers were first discussed by Barnoski

2

and Lotspeich of HRL at the 1976 Integrated Optics Conference in Salt Lake City, Utah, as a result of this program's efforts. Scattering into the m-line of the output mode pattern occurs as high optical power densities above a critical input power density are coupled into the waveguide layer for TE mode propagation along the x-axis of a y-cut sample. This scattering into the m-line is catastrophic with respect to any modulator application. We have observed, however, a "burn-in" phenomenon at room temperature which is quite interesting. With continuing input coupling we have observed that a return to a condition with no damage occurs (thus the signification "burn-in"). The nature of this burn-in phenomenon is explainable along the lines of the model of optical damage in the bulk.

We have shown during the course of this work that optical power levels at 5145 $\overset{\circ}{A}$ of >300 mW may be coupled into the waveguide layer with no optical damage and no output power saturation. This represents the state-of-the-art in optical waveguide modulator performance in that these are the highest optical power levels propagated in an optical waveguide structure in an active modulator configuration for visible wavelength operation. The optical damage is controlled by heating to 150°C where the self-annealing of any damage occurs due to the de-trapping of photo-electrons due to thermal excitation occurs. These results thus show that an approach to the low power high data rate modulator under development has been satisfactorily proven. A concentrated effort to boost the net input and output coupling efficiency of 44%, to a value close to the theoretical values of 90% is suggested as an important problem area where further work should be done.

SECTION II

WAVEGUIDE FORMATION

A. ## The Selection of an Appropriate Waveguide Formulation Technique

Planar thin film waveguides have been fabricated in a wide variety
of forms using such techniques as sputtering, epitaxy, photoresist spin-on
single crystal fine lapping, ion implantation and diffusion. Of these
different approaches to waveguide formation the approach most compatible
with low loss waveguide formation and the preservation of the excellent
electro-optic properties of $LiNbO_3$ and $LiTaO_3$ is that of diffusion. Wave-
guides may be formed in $LiNbO_3$ or $LiTaO_3$ by out-diffusion of Li_2O near
the surface of a polished oriented plate of $LiNbO_3$ or $LiTaO_3$.[2] An opposite
approach is to in-diffuse transition metal ions to form a high index region.
The latter approach has been incorporated into modulator design and
development, it is however instructive to review the out-diffusion process
to appreciate the choice of in-diffusion as the preferred technique.

A depleted concentration of Li_2O near the surface of a polished
oriented plate of $LiNbO_3$ and $LiTaO_3$ results in an increase in the
extraordinary index n_3 where

$$\frac{dn_3}{dX} = -1.63 \text{ for } LiNbO_3, \quad \frac{dn_3}{dX} = -0.85 \text{ for } LiTaO_3$$

and X is the fractional concentration of the out-diffusion component
$(Li_2O)_x(M_2O_5)_{1-x}$. Refractive index distributions of out-diffused guides
are well represented by a complementary error function

$$\Delta n_3 = A \text{ erfc } (d/B)$$

where A and B are functions of time and diffusivity and d is the distance
below the crystal surface. The typical values of these constants are
$A = 10^{-3}$ and B = 200 μm for samples heated in vacuum at 1100°C for about
20 hours.

5

The technique of metal indiffusion involves the diffusion process wherein a thin layer of metal such as titanium, niobium or copper is deposited upon a clean, polished crystal and subsequently allowed to diffuse into the crystal at high temperatures. The resulting index profiles are represented by a Gaussian form[3]

$$\Delta n = A' \exp(-x^2/4B'^2)$$

For this method the appropriate values of A' and B' are A' = 0.02 and B = 3 μm.

This comparison of the resulting diffusion caused index profiles focuses on the essential reasons for the selection of indiffusion as the process of waveguide formation: higher index of refraction changes at the surface and closer confinement of the optical fields to regions (≃3 μm deep) near the surface of the substrate. This makes the performance of a modulator based on the fringing electric fields of an interdigital electrode array quite efficient.

B. **Waveguide Formation Process**

Basically the formation of optical waveguide layers in LiTaO$_3$ involves the evaporation of a Ti metal film onto a polished LiTaO$_3$ substrate and the indiffusion of the Ti into the LiTaO$_3$ substrate. It is of utmost importance that this process be carried out in a reproducible and closely controlled manner. To this end a processing sequence was developed during this program whereby close scrutiny of the processing parameters such as surface quality, optical flatness, cleanliness, uniformity and adherence of the metal films to the substrate through the process was achieved. This processing sequence is listed below.

Processing Sequence of LiTaO$_3$ Substrates

(1) Clean for inspection - remove existing lapping compound and waxes with organic solvents and wipe surface clean.

(2) Check for flatness - use interferometer to measure the number of fringes across surface.

(3) Photograph with metallurgical microscope in both transmission and reflection - determine surface quality after polishing noting scratches, pits and cracks.

(4) Clean samples again.

(5) Deposit Ti metal - perform under vacuum (5×10^{-7} Torr) with e-beam heating.

(6) Oxidize Ti metal to TiO_2. Heat to 450 to 600°C for >4 hrs in O_2 atmosphere. Check surface subsequent to oxidation to check if metal lifted off the surface.

(7) Carry out diffusion - heat at 300°C/hr to temperature. Soak at temperature and cool down to 300°C/hr. Pole sample during cooling.

(8) Examine surface subsequent to diffusion. Note especially surface quality (whether milky film exists).

(9) Check flatness again - inspect for warping of the samples. This warping prevents use of prism coupling.

It has been found that the inclusion of the oxidation step (No. 6) prior to diffusion enhances the surface quality of the sample and the reproducibility of the process. Samples with thicknesses of >1.5 mm were found to be much less susceptible to warping than thinner samples and only samples with >1.5 mm thickness were subsequently used. Fast heating and cooling was found to be important to prevent sample cracking. The optimum temperature at which diffusion is best carried out is dependent on the film thickness and desired waveguide mode content of the structure. Single mode operation is, of course, the optimal manner in which the modulator structure should be implemented, so that the minimum temperature of diffusion for which good surface quality and low loss waveguide layers may be formed should be used. It has been found that for 500 Å films, for instance, the minimum temperature is used (>1300°C) a melting of the surface occurs. This melting has been directly observed using a novel furnace design which allows direct viewing of the sample throughout the oxidation and diffusion process. A minimum time of diffusion at 1250°C was found to be 4 hours for 500 Å films. To demonstrate that single mode guides may easily be formed by this in-diffusion process 200 Å and 50 Å thick films were used as Ti sources. For these thicknesses 1150°C

7

is quite sufficient to ensure excellent quality of the waveguide surface. For 200 Å films diffused for 4 hrs, two TE modes are found for 1150°C diffusion, and for 50 Å films single mode waveguides formed after 3 hrs diffusion at 1150°C for propagation along the x-axis of y-cut LiTaO$_3$ samples.

SECTION III

WAVEGUIDE PROPAGATION STUDIES

A. Prism Coupling

Excitation of the waveguide modes in $LiTaO_3$ waveguides formed by Ti-indiffusion was carried out by the prism coupling technique. In this technique a resonant coupling to waveguide modes occurs when phase matching conditions are met. The energy transfer from free propagating beams to guided optical beams occurs by way of frustrated total internal reflection. In our experiments TiO_2 and $SrTiO_2$ prisms were used. Special prism holders were constructed which would bring the coupling prisms and the diffused substrate surface into close optical contact. To localize the contact pressure between the sample and prism a local pressure point was formed below the sample. For high temperature experiments Teflon ridges were used which have performed satisfactorily at $\simeq150°C$.

Theoretical analyses of the prism coupling technique indicate that the maximum efficiency for input couplers is $\simeq80\%$ and for output couplers is close to 100% for uniform air gap coupling. A tapered gap can however yield close to 100% coupling efficiency for both input and output coupling.[4] In our experiments an average input coupling efficiency that has been measured is 55% as indicated by the dip method. In this method the percentage change in the return beam power as the coupling angle is tuned in and out of the coupling resonance angle is measured and this gives a direct measure of the coupling efficiency. Our estimates of the output coupling efficiency show that the coupling efficiency achieved using the localized pressure point prism couplers is greater than 80%. It is felt that much improvement in the modulator throughput can be made by concentrating on the construction of variable gap prism couplers.

B. Waveguide Mode Spectra and Index of Refraction Profiles

The measurement of the propagation constants of the various waveguide modes may be used to infer basic parameters about the profile of in-diffused species. An analysis of the expected mode indices for an assumed parabolic shape of the Ti-metal concentration (and therefore the index of refraction profile) is now given. This method if useful in multimode waveguide structures

9

where a theoretical fit of the observed mode indices yields the surface
index discontinuity as well as the effective depth d of the index of
refraction profile.

It is expected from diffusion theory that the Ti concentration
subsequent to diffusion should follow a Gaussian distribution and that
the index of refraction should also be given by the Gaussian form:[3]

$$n = n_0 (1 + \Delta e^{-x^2/d^2})$$

where Δ is the surface index discontinuity relative to n_0 or simply $\Delta n_0/n_0$,
n_0 is the substrate index, and d is the Gaussian diffusion depth parameter
equal to $2(Dt)^{1/2}$, where D is the diffusion constant and t is the diffusion
time. If we let n' be $n_0(1 + \Delta)$ and assume that the regions of interest
are those regions where $\frac{x}{d}$ is less than unity, we obtain an expression for
n which follows a parabolic profile:

$$n = n'(1 - \Delta \frac{x^2}{d^2}) \quad \text{for small } \Delta.$$

Marcuse[2] has calculated the modes of propagation in an index profile
of symmetrical behavior $n(x) = n(-x)$. We simply need the odd modes of
Marcuse's analysis since we may safely assume the electric fields at the
surface to be zero due to the large index difference. Thus our results
for the theoretical mode index of the mth mode is:

$$n_m^2 = n'^2 - \frac{4(m + \frac{3}{4})(2\Delta)^{1/2} n_0}{d K}$$

where $K = \frac{2\pi}{x}$ for m = 0, 1, 2...

Our experimental results for TE mode waveguide propagation along the
x-axis of y-cut $LiTaO_3$ substrates on a diffused sample with 5 modes were
compared with theoretical estimates of the mode indices based on fitting
the measured mode indices to the best Δ and d. The mode indices as
measured are always higher than those calculated using this analysis.
This is consistent with the view that a parabolic profile decreases more
rapidly than the Gaussian profile to the value of the substrate index. The
values of 0.012 for Δ corresponding to an index discontinuity at the surface

of the sample of 0.026 and the value of 3.5 μm for d are indicative of the magnitude of these parameters obtained in most diffused waveguide samples with multimode content. This sample was diffused at 1350°C for 12 hrs and had a 500 Å Ti coating. For single mode guides this kind of analysis of course does not work. However an indication of the depth of the diffusion for single mode structures may be obtained from microprobe analysis. For a sample diffused ≃4 hrs at 1075°C which had 500 Å Ti on the surface a microprobe measurement was performed. The results of this experiment are shown in Fig. 1. It is thus certain that single mode structures are formed with ≃2 μm thick waveguide layers. This small value of the waveguide thickness is crucial to efficient modulation of the guided beams using the fringing fields of interdigital electrode arrays.

C.   Waveguide Loss Measurements

Measurements were made of the waveguide losses at 5145 Å by varying the position of the output coupler prism relative to the fixed input coupler and measuring the output power as a function of separation of the two prism couplers. A semi-log plot of the output versus position showed that a clear straight line trend was readily obtained and that the problem of the assuring constant coupling throughout the measurement was avoided. The measured waveguide loss at 5145 Å for a TE mode of a two mode structure was 5 db/cm. This corresponds to an 20% (1 db) loss of power for propagation of the guided beam between prisms, which are spaced 2 mm apart. This thus represents an achievement of our original estimates of the waveguide loss at 5145 Å for this program.
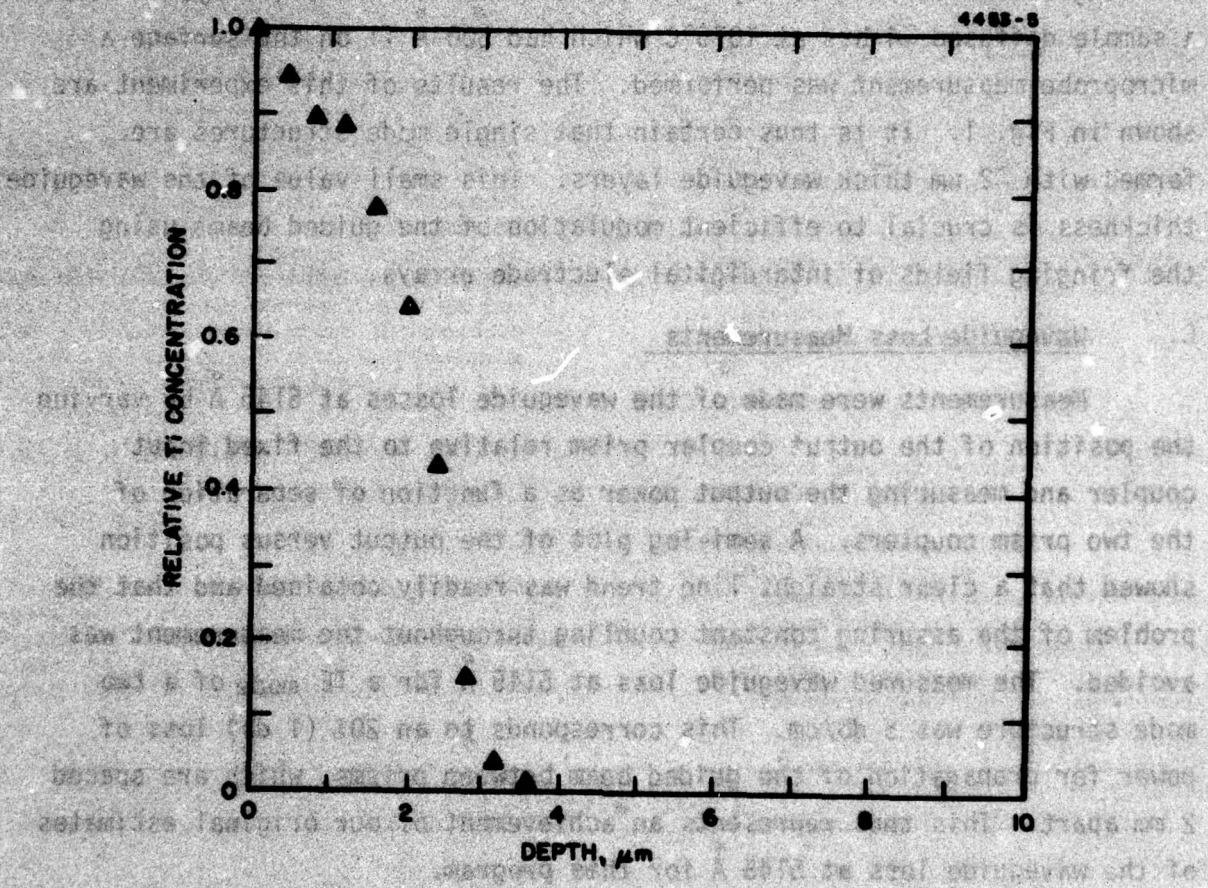
11

Fig. 1. Titanium concentration profile in LiTaO$_3$ from microprobe measurements.

SECTION IV

OPTICAL DAMAGE IN LiTaO$_3$ WAVEGUIDES

A. Model of Optical Damage in Bulk Crystals

When electro-optic crystals such as LiNbO$_3$, KTN and LiTaO$_3$ are exposed
to light of visible wavelength refractive index changes may occur. These
changes occur as a result of the build-up of local electric fields in the
material caused by the optical irradiation. The index of refraction change
is attributed to the redistribution of photoexcited carriers in the lattice
which results in a macroscopic polarization change and hence an index change
via the electro-optic effect. The photo-electrons are excited from impurity
traps by the incident radiation and, upon migration, are retrapped at other
locations, giving rise to the frozen-in electric field. In undoped crystals
the traps are due to small traces of impurities most notably Fe, Cu and Mn
for LiTaO$_3$ and LiNbO$_3$. The carrier migration occurs under the simultaneous
effects of diffusion forces and an electric field. This electric field may
be internal or applied. The relatively large size of the r_{33} electro-optic
coefficient for LiTaO$_3$ and LiNbO$_3$ compared with the other coefficients cause
the component of the space charge field along the optic axis (the z-axis)
to be most effective in changing the index of refraction. In particular
the extraordinary index of refraction changes due to this field E according
to

$$\Delta n_e = - \frac{1}{2} \eta_e^{\,3} r_{33} E$$

where η_e is the extraordinary refractive index, r_{33} is the third diagonal
component of the electro-optic tensor and E is the electric field along
the optic axis. This decrease of the index of refraction causes the optical
beam passing through a bulk modulator to diverge and the birefringence change
also affects the modulator performance. The optically induced changes in
the indices of refraction are observed to fade in a few hours but the
remaining part stays essentially unchanged for days when the light is
removed, unless the crystal is heated to ≅150°C.

LiTaO$_3$ is known to be much less susceptible (approximately two orders of magnitude less) to optical damage than LiNbO$_3$. Tsuya[3] has studied the dependence of the damage sensitivity on nominal impurity concentration, poling procedures, and heat treatment, and the dependence of the thermal decay and the distribution coefficients of different transition metals in LiTaO$_3$. Using electron paramagnetic resonance (EPR) and optical spectra studies it was found that Fe^{2+}, Cu^+ and oxygen vacancies, which occur as a result of reduction of the crystal or deviations from stoichiometry are the donor species, and that Fe^{3+}, Cu^{2+}, Mn^{3+} and V^{3+} are the trapping centers. The migration of oxygen vacancies during poling affects the damage susceptibility significantly. The oxygen vacancies migrate during poling from the positive electrode to the negative and the distribution of oxygen vacancies was found to be similar to that of the optical damage susceptibility in undoped crystals. The damage sensitivity in an Fe-doped crystal is two orders of magnitude larger near the negative electrode than near the positive electrode as a result of the poling. The optical absorption is also dependent on the poling conditions and the oxidation state of the sample. A marked difference in optical density of Fe-doped LiTaO$_3$ is seen between different crystal areas resulting from the poling process and resulting from the oxidation/reduction treatment. It was found that areas close to the positive electrode in fully oxidized oxygen vacancies of LiTaO$_3$ is found to determine to a large extent the sensitivity to damage in undoped LiTaO$_3$ crystals. The maximum damage threshold of bulk LiTaO$_3$ was reported to be $\simeq$10 kW/cm^2.

B.   Optical Damage in LiTaO$_3$ Waveguide - Room Temperature

Barnoski and Lotspeich[5] were the first to report the observation of optical damage in optical waveguides in LiTaO$_3$. This work was a direct result of this program's effort. The particular samples studied had a starting Ti layer thickness of 500 Å and were diffused in an O$_2$ atmosphere for 3 hrs at 1073°C. For TE mode propagations along the x-axis in a y-cut crystal the behavior of the output spot and the m-line scattering

14

was studied as high optical powers at 5145 Å were coupled into the waveguide structure. Examination of the output beam, displayed on a white screen, disclosed the following developments as the laser input power was increased. With reference to Fig. 2, an appreciable level of forward scattering first appeared at an input power of ∿240 mW. After the power was raised to a level of ∿600 mW, nearly all the output power was scattered into the m-line. However, as also illustrated in Fig. 2, the amount of scattering into the m-line decreased with time; and after ∿45 minutes, the quality of the transmitted beam with respect to the power scattered into the m-line returned to its original form as exhibited at low power levels. Following this observation, the resonance coupling angle was returned for maximum transmission, a change in resonance coupling was noted, and only one mode instead of two was observed.

The phenomenon is consistent with the present model of optical damage in bulk $LiTaO_3$ crystals. The m-line scattering is explainable as being due to the photo-induced index changes which reduce the value of n_e, the extraordinary index of refraction. The "burn-in" phenomena is due to the development of a steady state condition in which a constant index of refraction change is achieved under the cw laser radiation.

The optical damage in multimode $LiTaO_3$ waveguides was studied. These waveguides were diffused at high temperatures >1200°C to form deep waveguide layers of 4 to 5 μm. The waveguide supported 5 modes and the optical damage phenomena in the less tightly confined higher order modes were studied at room temperature. The effect of reduction in the optical power density in the higher waveguide modes was expected to yield less susceptibility to damage at room temperature. This was confirmed experimentally, however, optical damage as well as output power saturation still occurred. While a complete "blow-out" of the central mode spot into the m-line is avoided in these waveguide structures an elongation of the central spot 3 to 4 times its initial diameter along the m-line direction is observed and saturation of the output power at a maximum of 40 to 50 mW for 600 mW input power is observed. These results suggest the present room temperature results are unsatisfactory for incorporation into a final modulator design.
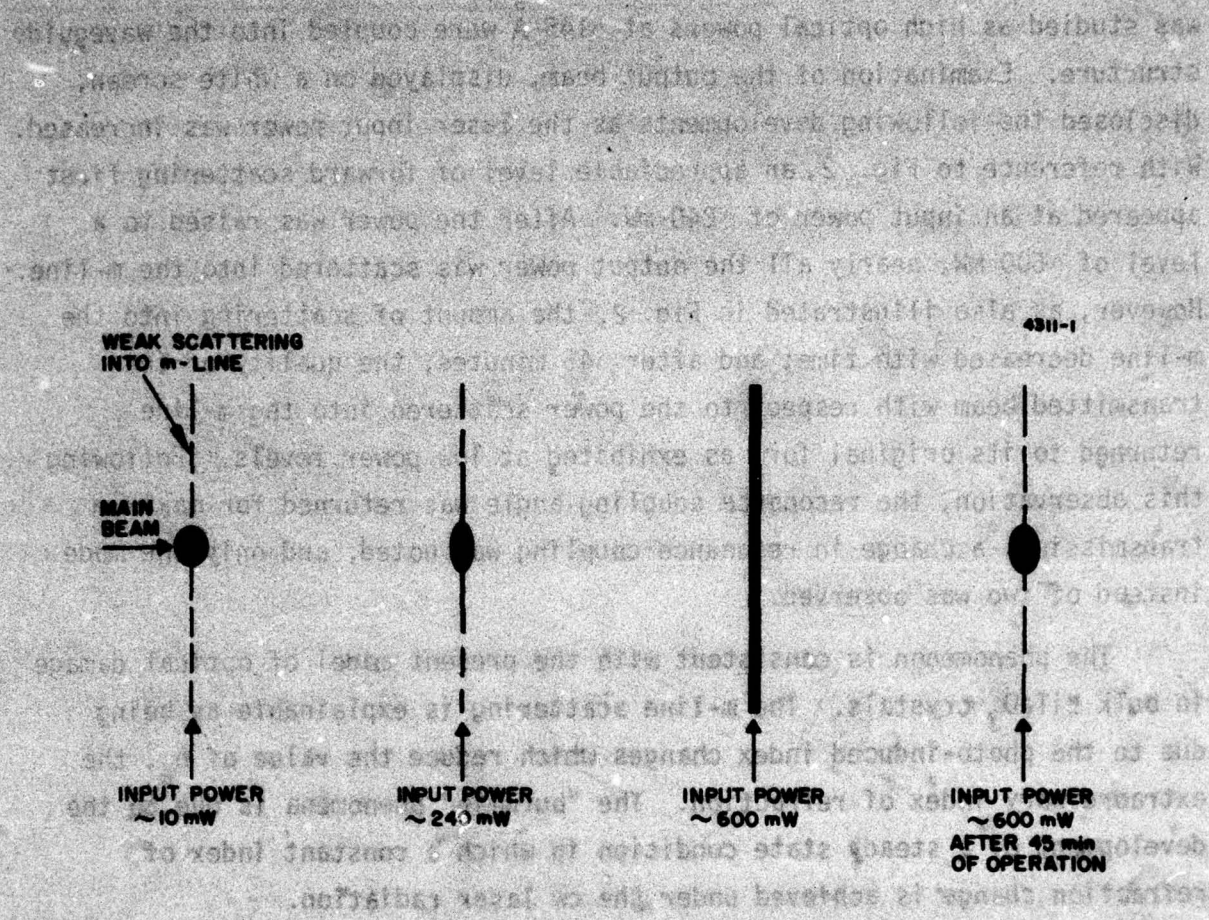
Fig. 2. History of output beam characteristics at 0.5145 μm as a function of input power and time.

C.   Optical Damage in LiTaO$_3$ Waveguide-Elevated Temperature

A property of the optical damage in bulk crystals is that the damage may be erased by heating to ≃150°C was utilized in a study of the optical damage in LiTaO$_3$ waveguides at these temperatures. A special heating stage and prism coupler apparatus was constructed for this purpose. The two samples which were studied most extensively were samples 21-A and B. These two samples exhibited excellent processing results. The Ti film (200 Å) deposited was quite uniform and did not have a pitted appearance. Subsequent to oxidation at 650°C for 24 hours and diffusion at 1100°C for 12 hours (21-A) and for 6 hours (21-B) excellent optical surfaces of the final waveguide structures resulted. Both samples have waveguide layers which support only 2 TE modes at 5145 Å for propagation along the x-axis and 1 TE mode for propagation along the z-axis. It is worth noting that only one mode was observed for propagation along a direction ≃45° with respect to the z-axis. This is close to the direction of optimum electro-optic modulation in a y-cut plate of ≃51° with respect to z-axis for LiNbO$_3$ and LiTaO$_3$.

The samples were first studied at room temperature with low laser input (25 mW) and the mode structure recorded. At this low level of power coupled into the waveguide no optical damage was observed and the optical waveguide modes could be easily studied. Estimates of the surface change in index of refraction and the diffusion depth for these samples are $\Delta n = 0.02$ and $d = 2.5$ μm, based on an analysis similar to that given in section II.

The samples and the prism coupler apparatus were heated to 150°C and high optical power studies carried out. No optical damage was observed with up to 216 mW coupled out of the waveguide; in addition, no saturation of the output power was observed as a function of input power.

To illustrate the evolution of the optical power level at different points within the waveguide structure, a detailed account is given in Fig. 3. The prism couplers are made of TiO$_2$ which has a reflectivity of
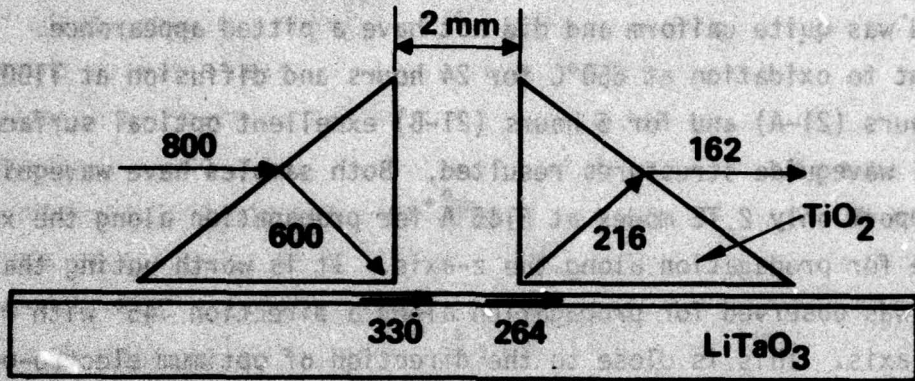
Fig. 3. Evolution of optical power through the waveguide structure. An estimated input coupling of 55% was used, resulting in a calculated 30% output coupling. Waveguide losses are estimated to be 5 dB/cm.

0.25 at 5145 Å. The waveguide loss in these layers has been estimated to ~5 dB/cm, which introduces a reduction of 20% of the power coupled into the fiber after propagating the 2 mm distance between prisms. An input prism coupling efficiency of 55% has been used as a reasonable estimate of this coupling strength based on measurements made by the "dip" method. This apportionment of the measured 44% net efficiency is consistent with the observation that a large fraction of the optical power in the waveguide film is efficiently coupled out with the new holder apparatus. The fact that no power saturation is observed is evidenced by the plot of output power as a function of input power for sample Ti-21B which is given in Fig. 4. It is important to note that the coupled input power density corresponding to 330 mW is ~17 kW/cm^2 which is above the room temperature damage threshold of 10 kW/cm^2 for LiTaO$_3$. These results are representative of the present state of the art in optical waveguide modulators structure designed for high optical power (>100 mW) handling power applications. The limit of 600 mW incident on the input coupling face may be raised by anti-reflection coatings of the input face of the prism. Both input and output prisms have recently been anti-reflection coated and tests of the throughput at higher incident energies will be made.
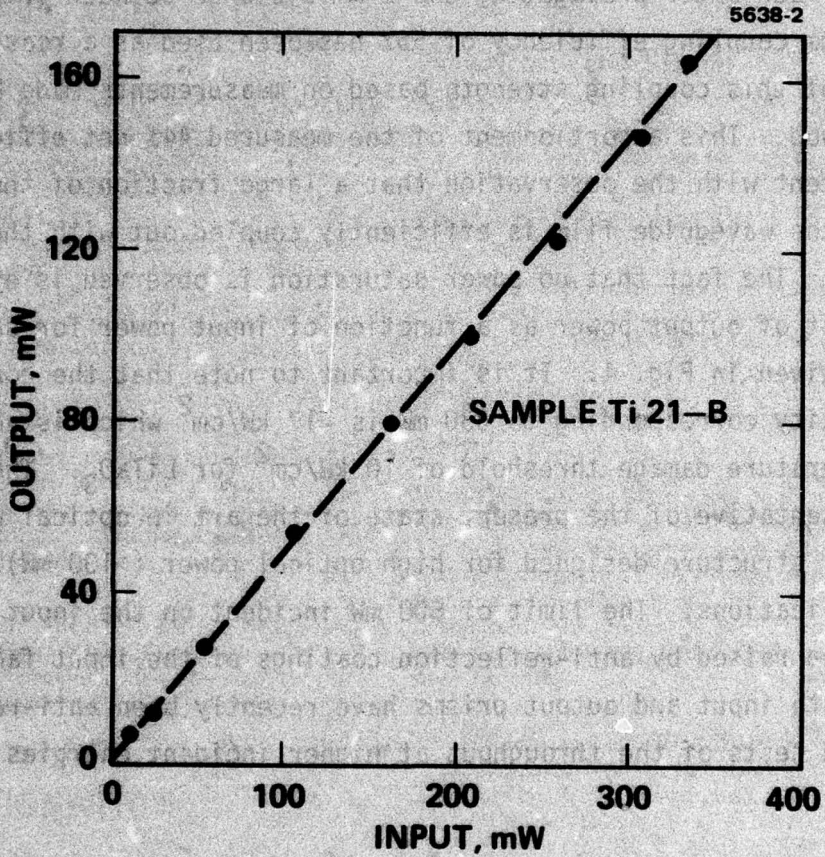
Fig. 4. Output power versus input power with 55%
input coupling efficiency. Sample Ti 21-B,
200 Å Ti metallization, 650°C for 6 hours
oxidation, 1100°C for 18 hours diffusion,
λ = 5145 Å; Stage temperature = 180°C.

SECTION V

MODULATOR DESIGN CONSIDERATIONS

A.   Electro-Optic Effect

The phase change ϕ, in radians, induced by the electric signal field over a path length L is

$$\phi = \frac{2\pi L}{\lambda_o} \Delta n \tag{1}$$

where Δn is the refractive index increment due to the electro-optic effect and λ_o is the free-space wavelength. The strongest interaction in $LiTaO_3$ and $LiNbO_3$ occurs when the applied electric field and optical electric polarization are both parallel (or nearly parallel[3]) to the crystalline c axis (optic axis). For this condition[6]

$$\Delta n_3 = \frac{1}{2} n_3^3 r_{33} E_3 \tag{2}$$

where n_3 is the extraordinary refractive index, r_{33} is the appropriate electro-optic coefficient, and E_3 is the applied electric field. Combining (1) and (2), we have

$$\phi = \frac{\pi L n_3^3 r_{33} E_3}{\lambda_o} \tag{3}$$

The crystal must be cut with its c axis in the plane of the waveguide essentially transverse to the beam propagation direction and the propagating optical mode must therefore have TE polarization. This polarization has the best loss characteristics in proximity to the metal electrode surfaces.

Table I lists the relevant electro-optic and dielectric characteristics of $LiTaO_3$ and $LiNbO_3$ for reference and comparison. The prefixes (T) and (S) stand for unclamped, or constant stress, and clamped, or constant strain conditions. The dielectric constants or specific permitivities are indicated by $\varepsilon_1/\varepsilon_o$ and $\varepsilon_3/\varepsilon_o$, normal and

21

TABLE I
Electro-optic Materials Properties

5853-6

QUANTITY	LiTaO$_3$		LiNbO$_3$	
	0.53 μm	1.06 μm	0.53 μm	1.06 μm
n_3	2.21	2.14	2.23	2.16
(T)r_{33}, 10^{-10} cm/V	~ 31	~ 29	32.2	~ 32
(S)r_{33}, 10^{-10} cm/V	30.3	~ 29	30.8	~ 30
(T)$n_3^3 r_{33}$, 10^{-9} cm/V	33.5	~ 28.4	35.7	~ 32
(S)$n_3^3 r_{33}$, 10^{-9} cm/V	32.7	~ 28.4	34.1	30
(T)ϵ_1/ϵ_0	51		78	
(S)ϵ_1/ϵ_0	41		43	
(T)ϵ_3/ϵ_0	45		32	
(S)ϵ_3/ϵ_0	43		28	

(T) = UNCLAMPED
(S) = CLAMPED

parallel to the optic axis, respectively, where ϵ_0 is the permittivity of free space. We note the large change in ϵ_1 for $LiNbO_3$ in going from the unclamped to clamped condition. This has an adverse effect on the frequency response characteristics. Likewise, the change in r_{33} is substantially greater than that of $LiTaO_3$, which similarly has a stronger effect upon the electro-optic frequency response. For Bragg diffraction the zero[th] and first-order powers are proportional respectively, to $\cos^2(\phi/2)$ and $\sin^2(\phi/2)$. For full modulation, corresponding to 100% depletion of the zero-order beams in the idealized cases, the maximum required values of ϕ is $\phi_{max} = \pi$.

B.   Design Calculations

In order to design a suitable diffraction modulator we need to determine allowable dimensions of the electrode array, the resulting capacitance, required shunt resistance, and suitable matching transformer under the primary constraint of a driver power not exceeding 3 W from a 50-Ω source and a minimum bandwidth of 500 MHz. It turns out that this can be done in a fairly straightforward manner, and that in particular, both the power and the capacitance can be uniquely expressed in terms of the ratio of electrode separation to electrode length, s/L.

With optimized video peaking the power required to drive a capacitance C over a bandwidth B with peak driver voltage V_m is

$$P = \frac{V_m^2}{2R_s} \simeq \frac{\pi}{2} BCV_m^2 \tag{5}$$

where $R_s \simeq 1/\pi BC$ is the shunt resistance needed to dissipate the power and provide an RC-limited bandwidth B. The capacitance of an inter-digitated electrode array having N finger pairs on an x- or y-cut uniaxial crystal such as $LiTaO_3$ is[7]

$$C = \left[\epsilon_0 + (\epsilon_1\epsilon_3)^{1/2}\right] KLN \ . \tag{6}$$

23

In this formula, K is the correction factor[8] determined from the ratio of electrode width to spacing, w/s. For LiTaO$_3$ in the clamped condition (which is expected to obtain over most of the operating band)

$$C = 3.8 \text{ KLN} \quad pF. \tag{6'}$$

The number of electrode pairs is readily determined from a knowledge of the total width of the electrode array. For an input laser beam having a $1/e^2$ diameter D equal to about 1 mm, it is sufficient to assume an electrode array width of 1.5D. Thus,

$$N = \frac{1.5D}{S} = \frac{0.15}{S} \tag{7}$$

where S is the periodicity, expressed in cm. S is subsequently expressed as a multiple of the electrode spacing s.

The applied electric field E$_3$ in the active region of the beam is estimated to be approximately[9]

$$E_3 = \frac{V_m}{2s} \tag{8}$$

when the distance below the surface is comparable to s. This is the assumed design condition which leads to uniform field strength across the optical beam. It is convenient to express V$_m$ in terms of a commonly used electro-optic parameter E$_3 \cdot$ L, the so-called field-length product. Thus, from (8)

$$V_m = 2(E_3 \cdot L)\left(\frac{s}{L}\right) \tag{9}$$

where

$$E_3 \cdot L = \frac{\phi_{max}\lambda_o}{\pi n_3^3 r_{33}} \tag{10}$$

according to Eq. (3), and ϕ_{max} is given in (4). With a specific electrode width-to-spacing ratio, it is easy to see from (6') and (7) that the capacitance is proportional to L/s and from (5) and (9) that the power is proportional to s/L.

We have calculated the design values of C, the electrode capacitance, R_s, the shunt resistance, S, the electrode period, N, the number of periods and Q, the Bragg diffraction parameter[10] $Q = \frac{2\pi\lambda_0 L}{n_3 S^2}$ for a 2.5 mm long (L) grating. These calculations were made subject to the constraint of 3 W electric drive power. The working equations for the LiTaO$_3$ modulator are given below. The results are shown in Fig. 5.

$$P = \frac{\pi}{2} BC V_m^2 = 3 W$$

$$V_m = 2(E_3 \cdot L)(s/L)$$

$$N = 1500/S = \frac{1500}{s} \cdot \frac{s}{S}$$

$$C = 0.57 \left(\frac{s}{S}\right)K\left(\frac{L}{S}\right) \times 10^{-2}$$

$$P = 4.616 \times 10^3 \left(\frac{s}{S}\right)K\left(\frac{S}{L}\right)$$

C.   Impedance Matching Considerations

It is imperative that careful consideration of the problem of impedance matching be done to determine the optimum electrode configuration. For a modulator with L = 2.5 mm, S = 19.4 μm and using K = 0.85, the electrode capacitance C is $\simeq$62 pf and $R_2 \simeq$ 10 Ω. An increase of the effective resistance by 4 and a decrease of the effective capacitance by 4 results if the electrode array is divided into 2 elements in series[8] as shown in Fig. 6.

The termination characteristics of this low power high data rate modulator design with C = 15 pf and R = 43 Ω has been studied. The reflection coefficient has been calculated using these parameters up to 500 MHz. The formulae used are:

$$\rho = |\rho|e^{i\phi} = \frac{Z_0 - R + jwZ_0 RC}{Z_0 + R + jwZ_0 RC} = \frac{7 + j(0.1013)f(MHz)}{93 + j(0.1013)f(MHz)}$$

where $Z_R = \frac{R}{1 + jwRC}$ and Z_0 = 50 Ω. The results are shown in Fig. 7. In addition the ratio of the coupled power V_C to the transmitted forward

25

Fig. 5. Modulator design calculation results as a function of electrode width-to-periodicity ratio w/S.
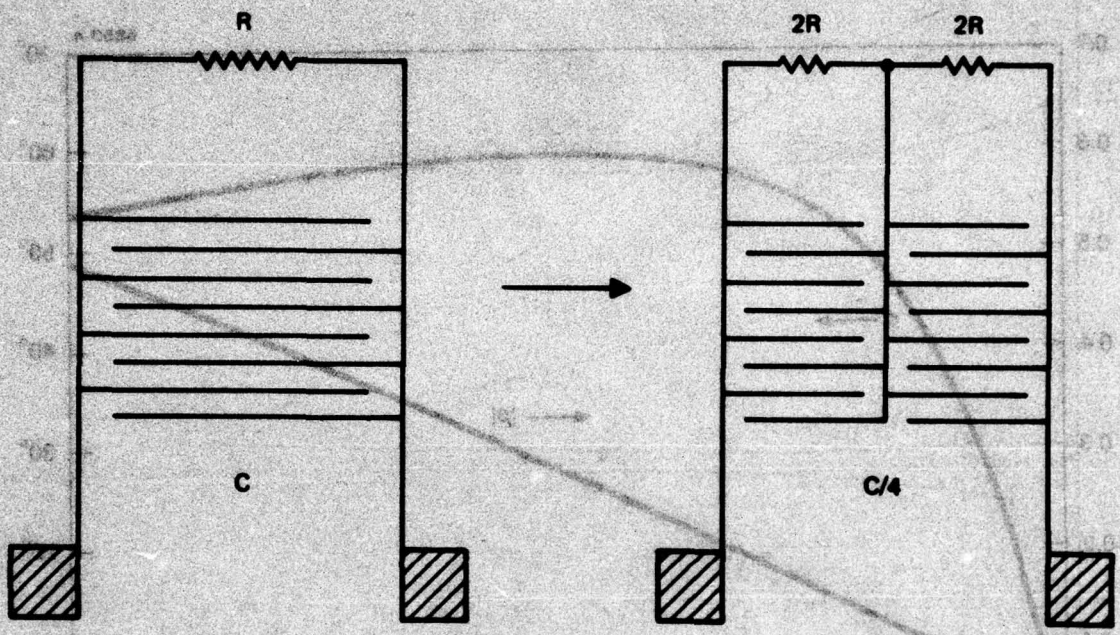
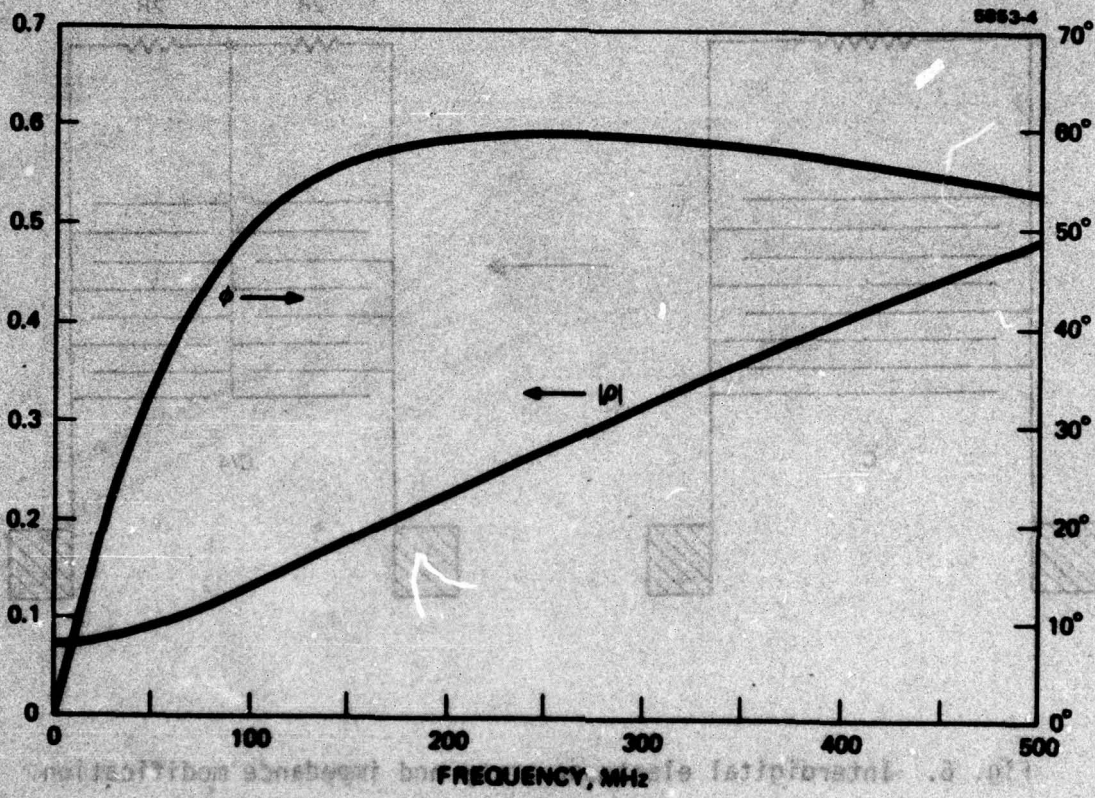**Fig. 6.   Interdigital electrode array and impedance modification.**

Fig. 7. The calculated reflection coefficient amplitude and phase.

power V_i has been calculated for various values of the lead inductances which may occur in the final device configuration. The results are shown in Fig. 8 along with the equivalent circuit used in the calculations. A schematic diagram of the modulator design is shown in Fig. 9.
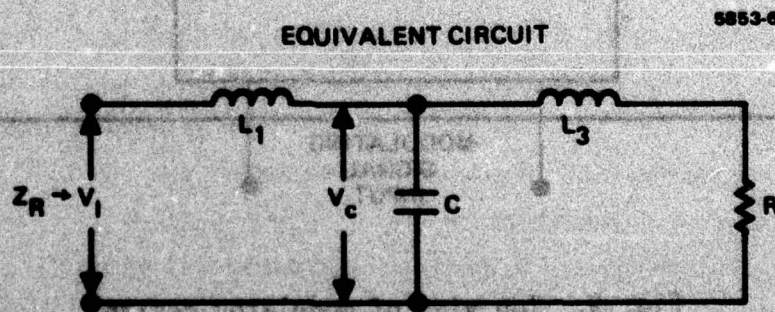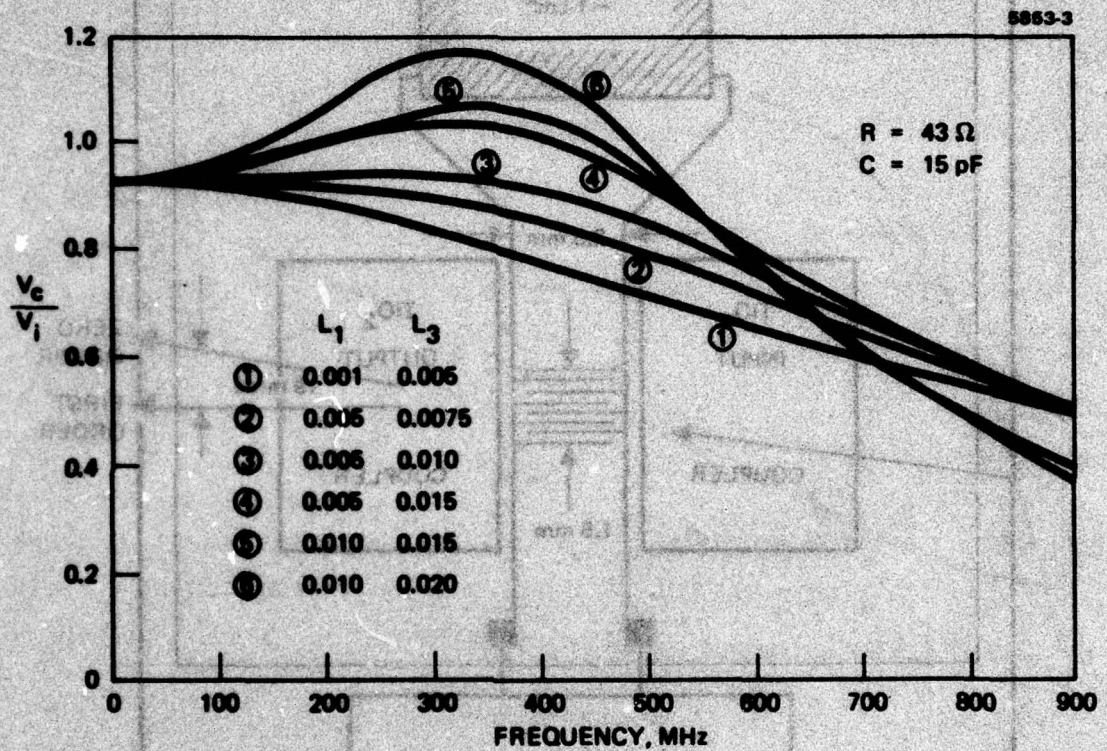

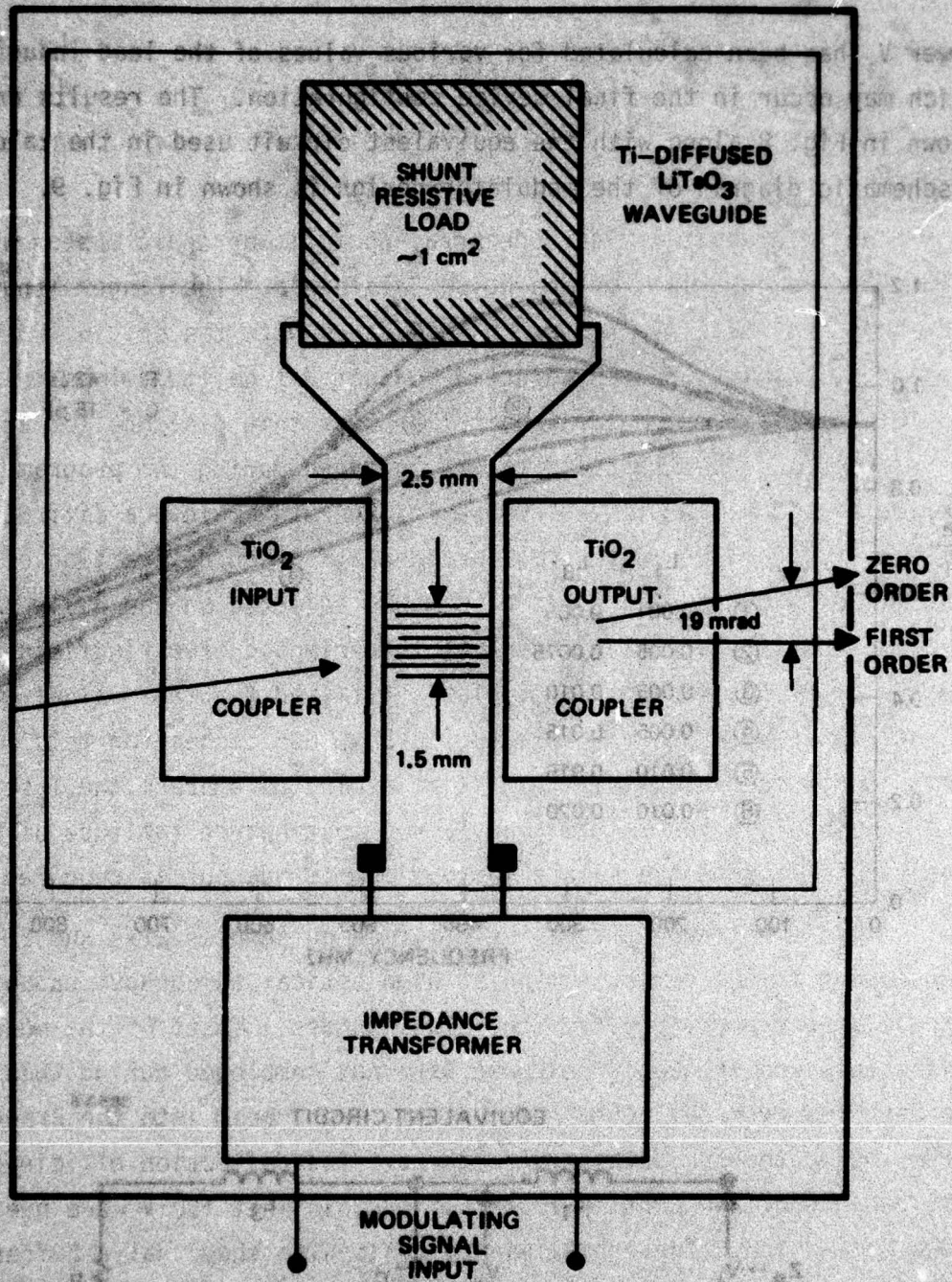Fig. 8. The frequency dependence of the coupled power for the modulator structure.

Fig. 9. Top view of modulator design.

SECTION VI

MODULATION FABRICATION

An interdigital electrode array photolithographic master was ordered from Electromask, Inc. of Van Nuys, California. The finger length chosen for this test mask was 2.0 mm in accordance with the original proposal design. The distance was selected so that a 1 db (20%) loss in power would result for waveguide propagation over this distance for an expected 5 db/cm loss. This loss figure was obtained during the program. The periodicity S = 0.8 mil was chosen in order to achieve a diffraction parameter $Q(=2\pi\lambda_0 L/n_3 S^2) = 10$, for adequate Bragg diffraction efficiency. The finger width-to-gap ratio of 2:3 was selected on the basis that a minimum spatial harmonic content of the fringing electric field in the region of the guided optical field is attained for this value. The electrode array width was selected to be 0.236 inches for this mask. This is considerably wider than is necessary to embrace the laser beam but is useful in the initial modulation tests where latitude of beam positioning across the sample for optimum throughput is required.

Gold electrode patterns were formed on samples 21-A and 21-B subsequent to the demonstration of high optical throughput capabilities at elevated temperatures for these waveguides. Tests of the modulation efficiency and frequency response were not completed during this program. We have observed deflection of the zero order beam into the Bragg first order using these modulator structures. The deflection efficiency was low because of the grating imperfections, in that 150 V were needed for ≈30% deflection. These preliminary tests also show that a buffer layer will be needed to isolate the metal grating from the waveguide surface, there being a strong deflection at twice the Bragg angle due to the index changes caused by the metal grating above.

SECTION VII

CONCLUSION AND RECOMMENDATIONS

In conclusion it is felt that the work described in this report has documented the fabrication processing and testing of optical waveguide modulator structures in $LiTaO_3$ capable of handling high optical power levels (>300 mW) with <u>no</u> optical damage and <u>no</u> power saturation effects. This work has established the state of the art in optical power handling capabilities in waveguide modulators operating in the visible wavelength range. Several recommendations for further work may be made. The most important areas where significant improvement in the device performance may be accomplished is that of the prism coupling efficiency. By using variable gap couplers close to 100% coupling (<u>both</u> input and output) may be achieved. This would be a significant improvement over the set coupling efficiency of 44% (55% input and 82% output) achieved during this program. The use of the variable gap couplers will also yield an output beam with an intensity profile very close to a Gaussian beam profile. This will facilitate the incorporation of the waveguide modulator into the telescope system of the actual laser communication system being developed for the 405B program. Further improvements may be made in the throughput of the modulator by reducing the waveguide losses from the 5 db/cm level to <1 db/cm. At present the 5 db/cm loss for 5145 Å wavelength operation figure is consistent with the reported results of Hammer and Phillips[11] at RCA for $LiNb_xTa_{1-x}O_3$ waveguides of ~5 db/cm for wavelengths close to 5145 Å. <1 db/cm loss figure may be obtained. Lastly the power handling capability of these waveguide structures may be greatly enhanced (most especially the room temperature results) by using very pure $LiTaO_3$ substrates as starting materials. The reduction of the Fe content in $LiTaO_3$ is most important in reducing the damage susceptibility. Experimentation with high purity $LiTaO_3$ crystals should be carried out.

REFERENCES

(1)   P. K. Tien and R. Ulrich, J. Opt. Soc. Am. 60, 1325 (1970).

(2)   I. P. Kaminow and J. R. Carruthers, Appl. Phys. Lett. 22, 326 (1973).

(3)   J. M. Hammer and W. Phillips, Appl. Phys. Lett., 24, 545 (1974).

(4)   J. R. Harris and R. S.-abat, IEEE Trans. Microwave Theory Tech. MTT-9, 269 (1971).

(5)   M. K. Barnoski and J. F. Lotspeich, Proceedings of the Integrated Optics Conference, Salt Lake City, Utah (1976).

(6)   F. S. Chen, Proc. IEEE 58, 1440 (1970).

(7)   S. G. Joshi and R. M. White, J. Acoust. Soc. Am. 46, 17 (1969).

(8)   J. Noda, N. Uchida, and T. Saku, Appl. Phys. Lett. 25, 131 (1974).

(9)   M. A. R. P. deBarros and M. G. F. Wilson, Proc. IEEE 119, 807 (1974).

(10) W. R. Klein and B. D. Cook, IEEE Trans. Sonics Ultrason. SU-14, 123 (1967).

(11) J. M. Hammer, M. T. Duffy and W. Phillips, Final Report QRRL-74-CR-32, Contract No. N00014-73-C-0388, April 1974.